Available online at www.sciencedirect.com
SCIENCE DIRECT®
International Journal of Mass Spectrometry 244 (2005) 109–124
International Journal of Mass Spectrometry
www.elsevier.com/locate/ijms

Review

Gas-phase ion–molecule reactions of divalent metal complex ions: Toward coordination structure analysis by mass spectrometry and some intrinsic coordination chemistry along the way

M. Yajaira Combariza, Angela M. Fahey, Aleksandr Milshteyn, Richard W. Vachet *

Department of Chemistry, LGRT 701, 710 N. Pleasant St., University of Massachusetts at Amherst, MA 01003, USA

Received 20 April 2005; received in revised form 26 May 2005; accepted 31 May 2005
Available online 1 July 2005

Abstract

Gas-phase ion–molecule reactions of divalent metal complex ions are strongly affected by the coordination structure around the metal. This review describes how association reactions between reagent ligands and complex ions proceed to extents that depend upon a metal complex's coordination number, types of coordinating functional groups and coordination geometry. The coordination number of a metal complex affects its reactivity because complexes of divalent metal ions will add reagent molecule(s) to fill vacant coordination sites. The thermodynamics and kinetics of these reactions are very sensitive to both the types of functional groups bound to the metal and the geometry of the groups around the metal ion. Such a strong dependency on the coordination structure of a metal complex suggests that ion–molecule reactions might make mass spectrometry suitable for elucidating a metal's coordination structure. Given mass spectrometry's inherent sensitivity and the ability to carefully control reaction conditions in a mass spectrometer, ion–molecule reactions have the potential, both analytically and fundamentally, to provide greater insight into the chemistry of divalent metal complexes.

Keywords: Ion–molecule reactions; Quadrupole ion trap mass spectrometer; Divalent metal ions; Metal complex; Coordination structure

Contents

* Corresponding author. Tel.: +1 413 545 2733; fax: +1 413 545 4490.
E-mail address: rwvachet@chem.umass.edu (R.W. Vachet).

1387-3806/$ – see front matter © 2005 Elsevier B.V. All rights reserved.
doi:10.1016/j.ijms.2005.05.006

1. Introduction

It is axiomatic in chemistry that "structure controls function." For transition metal complexes, the function of interest is usually reactivity, and the structure that controls reactivity is coordination structure, which refers to the number, type and orientation of the ligand-donor groups around the metal center. A key role of this coordination structure is to tune the metal's electronic structure and by doing so mediate any bond making and bond breaking. Ligand structure around the metal can also influence chemistry via steric control.

The relationship between a metal complex's coordination structure and its chemical properties has led to the development of numerous spectroscopic techniques that can provide this structural information. These techniques include ground-state methods that use magnetic fields, valence excited-state methods that rely on UV or visible radiation and core excited-state methods based on X-ray radiation. This array of techniques has been developed because no one method provides all the desired information or is suitable for the analysis of every given complex. Special cases still arise in which traditional methods are unsuitable. One situation in which current methods often fail is when the complex of interest is present at very low concentrations. Under such conditions, most established techniques are unable to provide adequate signal for gathering the information of interest.

Because we are interested in studying the coordination structure of metal complexes present at trace levels in marine environments, we have begun to explore new ways to gather this information using mass spectrometry (MS). MS has in many ways revolutionized the analysis of peptides and proteins because of its ability to provide structural information while maintaining its exquisite sensitivity. A question that we have recently pursued is whether MS can similarly provide detailed structural information for metal complexes while maintaining this sensitivity. For organic ions structural information is typically obtained using a variety of dissociation techniques, including most often collision-induced dissociation (CID). For divalent metal–ligand complexes, structural information is often more difficult to obtain unambiguously using analytical CID [1–8] as it is performed during routine tandem MS (MS/MS) experiments on non-specialized mass spectrometers. Metal–ligand interactions are typically weaker than the covalent bonds in organic molecules, so collisional activation of metal complex ions can lead to the rearrangement of the metal center, resulting in dissociation chemistry that does not necessarily reflect the coordination environment of the metal. Furthermore, while the dissociation chemistry of a metal complex ion may still reflect its coordination structure in many cases, the relationship between the two is not always obvious. On the contrary, for small monovalent metal–ligand complexes, threshold CID measurements can provide very detailed thermodynamic information, and when combined with theoretical calculations, these measurements can also provide detailed structural insight [9–12]. Currently, though, threshold CID measurements are limited to monovalent metal ions, but applications of these methods to divalent metal ions will undoubtedly appear in the future [13].

An alternate approach to gather insight into divalent metal coordination structure is reaction of metal complex ions with neutral reagents at thermal energies. These thermal reactions are much less likely than dissociation-based techniques to disrupt an ion's structure, and these reactions usually generate product ion spectra that are much simpler to interpret. In addition, numerous potential reagents offer a broad scope of chemical reactions from which a complex's structure may be deciphered. The use of such ion–molecule (I–M) reaction chemistry relies on the idea that just as a complex's coordination structure affects its reactivity, so should a complex's reactivity reflect its coordination structure. This review will demonstrate ways in which our group has used gas-phase I–M reactions to provide varying degrees of detail about a divalent metal complex's coordination structure by choosing the appropriate reagent and collecting the proper experimental data. Furthermore, because these reactions are done in the gas-phase, some intrinsic coordination chemistry can be gathered at the same time. Of course, metal–ligand coordination chemistry is a very mature field, but studying the chemistry of divalent metal complexes without interferences from solvent or counterions can, in the very least, provide confirmation of well-developed theories (e.g. ligand field theory) especially for coordinatively unsaturated complexes. In other cases, new insight into divalent metal complex chemistry can be gathered.

2. Experimental methods

All of the experiments described in this review were performed on a modified Bruker Esquire-LC quadrupole ion trap mass spectrometer (QITMS). The instrumental modifications and the details of how the QITMS is used have been described elsewhere [14]. Briefly, metal complex ions are generated by electrospray ionization from solutions containing the complex of interest, and the ions are transferred via ion optics into the trapping volume of the QITMS. Ions of interest are then isolated in the gas-phase using supplementary waveforms applied to the endcap electrodes of the QITMS and allowed to react with neutral reagent gas(es) that are introduced into the vacuum system via a custom leak-valve system. Reaction times with reagent gases can range from 10 to 10,000 ms. The product ions formed from these reactions are then detected in a mass-selective manner by steadily increasing the rf voltage applied to the ring electrode while simultaneously applying a resonance ejection signal to the exit endcap electrode to enhance ion ejection to an electron multiplier.

3. Coordination structure

In the context of this review, coordination structure refers to the number, type and orientation of the ligands around a

given metal. Another very important aspect of a complex's structure is the electronic structure of the metal center, that is, the relative energy spacing and occupancy of the metal's 5 d-orbitals. It is not obvious how I–M reactions in a mass spectrometer might provide information about a metal's electronic structure directly; however, coordination structure certainly influences a metal's electronic structure. In this review, we demonstrate how I–M reactions are sensitive to a complex's coordination number, coordinating functional groups and coordination geometry.

3.1. Coordination number

Using I–M reactions to determine a metal complex's coordination number relies on the idea that metal complexes will react to an extent that depends upon their coordinative unsaturation. Indeed, the observation that coordinatively unsaturated metal complex ions react with neutral ligands in the gas-phase has been reported by several investigators [14–35]. We have demonstrated using two different approaches how I–M reactions can determine coordination numbers. The first approach involves reagent gases that are selectively reactive with complexes that have a given coordination number [16,21–23,27]. In previous work, with complexes having nitrogen-containing ligands, we showed that 6-coordinate complexes of divalent metal ions are generally unreactive, while 5-coordinate complexes react with reagents such as pyridine or ethylamine to add one reagent molecule. In addition to reacting with pyridine and ethylamine, 4-coordinate complexes react with ammonia and 3-coordinate complexes react with ammonia, water and methanol.

The ability of the more weakly electron-donating reagents (e.g. ammonia, water and methanol) to only form adducts with the lower coordinate complexes is explained by the nature of the gas-phase environment in the QITMS and by the lower electropositive character of the metal center in the complexes with higher coordination numbers. Reactions in the QITMS occur in the presence of ∼1 mTorr of He, which acts to effectively thermalize ions to a temperature that is close to the vacuum chamber walls [36–38]; in our experiments this temperature is about 300 K. These reactions occur over time periods that range from 10 to 10,000 ms. Ammonia, water and methanol evidently interact too weakly with 5- and 6-coordinate complexes to overcome the unfavorable entropy associated with adduct formation at 300 K. Similarly, the interactions between 4-coordinate complexes and water or methanol must also be too weak to overcome the unfavorable entropy associated with adduct formation. In other words, the magnitude of $T\Delta S$ exceeds the magnitude of ΔH, so these reactions are unfavorable (i.e. $+\Delta G$). Of course, several investigators have shown that divalent metal ions can be generated by ESI with solvent molecules that include ammonia, water and methanol, and these complexes can be analyzed by MS [39–48]. Even complexes with good nitrogen donors, such as bipyridine, can be generated with bound solvent molecules [49–51]. In these previous cases, though, the analysis time window was short and ion temperatures were very likely below 300 K, which enabled weakly bound solvent molecules to remain bound so that mass analysis was possible.

Selective reactions with different reagent gases can provide coordination number, but a more analytically convenient approach for determining this information is to use a single reagent that is capable of "titrating" the open coordination sites in a complex [14,34,35]. In this approach, the corresponding mass increase (or the absence of a mass increase) after the I–M reaction indicates the initial coordination number of the complex. An abundance of solution-phase and solid-state data suggests that divalent cations of the late first-row transition metals (i.e. Mn(II) through Cu(II)) have a tendency to form 6-coordinate complexes. Thus, if a metal complex ion has a coordination number less than six, then one might expect the ion to react with a neutral reagent gas to obtain a full coordination sphere. An example of this approach is shown in Fig. 1 for a series of 4-, 5- and 6-coordinate complexes of Mn(II), which were reacted with acetonitrile (pressure = $4.2 \pm 0.4 \times 10^{-10}$ atm) for 100 ms. The ligands bound to Mn(II) in these complexes are shown in Fig. 2.

3.1.1. Reagent gas considerations

Titration of the open coordination sites in a metal complex ion is possible when the appropriate reagent gas is chosen. For example, in our experience with well over 100 metal complex ions, ammonia, water, methanol and ethanol do not react significantly enough to form adducts with most 5-coordinate complexes, so these are not effective reagents for the titration experiments. Other reagent gases such as pyridine, ethylamine and acetonitrile, however, do form mono-adducts with most 5-coordinate complexes and form di-adducts with most 4-coordinate complexes.

While we have not thoroughly investigated the physicochemical properties necessary for a reagent ligand to effectively titrate a metal complex's open coordination sites, a few characteristics appear to be important. Table 1 shows the ionization potentials (IP), dipole moments (DM), gas-phase basicities (GPB) and polarizabilities of several reagent gases that we have studied. For almost all of the complexes studied, the addition of reagents such as pyridine, ethylamine and acetonitrile are kinetically and thermodynamically favored over the addition of ammonia, water, methanol and ethanol. The relatively high reactivity of pyridine and ethylamine is not unexpected given that these reagents are known to be relatively good ligands in solution. The relatively high reactivity of acetonitrile and low reactivity of ammonia, however, are somewhat surprising. Ammonia is usually considered a better ligand for divalent metal ions in solution than acetonitrile. There are two notable differences between acetonitrile and ammonia that may explain this observation. Differences exist between the magnitudes of their DMs (3.925 D versus 1.472 D) and polarizabilities (4.42 $Å^3$ versus 2.22 $Å^3$). Polarizability and DM are good indicators of a molecule's ability to

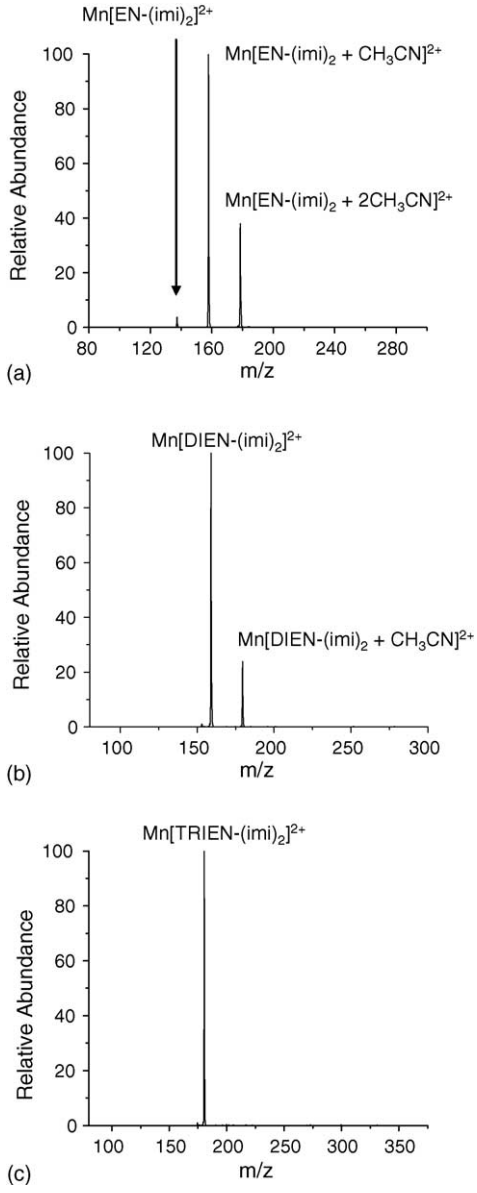

Fig. 1. Mass spectra obtained after reacting: (a) $Mn[EN\text{-}(imi)_2]^{2+}$, (b) $Mn[DIEN\text{-}(imi)_2]^{2+}$ and (c) $Mn[TRIEN\text{-}(imi)_2]^{2+}$ with acetonitrile (pressure = $4.2 \pm 0.4 \times 10^{-10}$ atm) for 100 ms.

donate electron density to a metal, and thus they appear to be good indicators of a reagent's intrinsic ligating abilities in the gas-phase. Clearly, though, the combination of DM and polarizability is not the only gauge of ligating ability as ethylamine has the lowest DM of the gases in Table 1, yet it is one of the more reactive reagent ligands. Ethylamine has a relatively high gas-phase basicity (GPB), which means it can readily donate a lone-pair of electrons. Pyridine also has a relatively high GPB, while having a high DM and large polarizability. In our experiments, pyridine typically forms the most kinetically and thermodynamically favorable adducts with metal complex ions, which suggests a high GPB, DM and polarizability are important characteristics of a strong ligand for divalent metal ions in the gas-phase. An inverse correlation

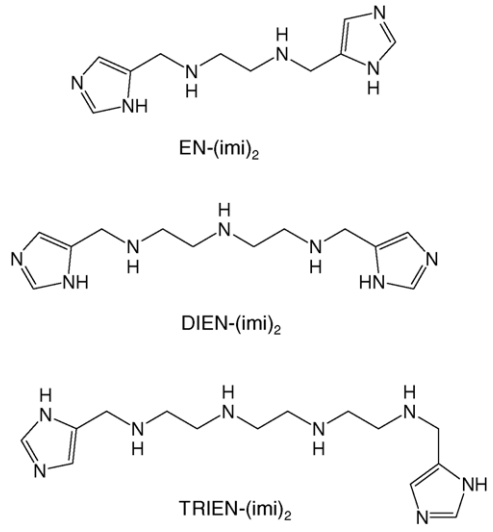

Fig. 2. Ligand structures for complexes whose reaction data are shown in Fig. 1.

between IP and reaction rates has been demonstrated previously for reactions between $C_5H_5Fe^+$ and various reagent gases [53], implying the importance of IP as an indicator of gas-phase ligand strength. While we do not have enough data to comment on the importance of IP, the favorable reactivity of acetonitrile indicates that this trend does not hold for the divalent metal complex ions that we have studied.

Titration as a means of determining a complex's coordination number is attractive because of its simplicity, but our experience shows that reactions that compete with simple ligand addition can complicate the experimental measurements. Because some of the good titrating reagents are strong bases, proton transfer can compete with ligation. An example in which proton transfer can occur involves the Mn(II) complex of the ligand AM-$(pyr)_2$ (structure shown in Fig. 3). Upon reaction of $Mn[AM\text{-}(pyr)_2]^{2+}$ (*m*/*z* 226.5) with pyridine, product ions at *m*/*z* 452 and *m*/*z* 80 are observed. Proton transfer is the dominant reaction observed and is possible because ligation of Mn(II) to the amine nitrogen of AM-$(pyr)_2$ reduces the basicity of this site. This complex is 6-coordinate, so it is not expected to form an adduct with pyridine, but if this complex's coordination number had been

Table 1
Ionization potentials (IP), gas-phase basicities (GPB), dipole moments (DM) and polarizabilities of several reagent gases

Reagent ligands	IP (eV)	GPB (kcal/mol)	DM (D)	Polarizability (Å^3)
Water	12.62	157.7	1.855	1.48
Methanol	10.84	173.2	1.70	3.23
Ethanol	10.48	178.0	1.69	5.11[a]
Ammonia	10.07	195.7	1.472	2.22
Ethylamine	8.7	210.0	1.22	4.11[a]
Pyridine	9.26	214.7	2.215	13.33[a]
Acetonitrile	12.20	179.0	3.925	4.42[a]

[a] These polarizabilities were calculated using the method of Miller and Savchik [52].

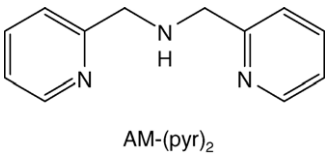

Fig. 3. Structure of AM-$(pyr)_2$.

unknown, the observed deprotonation reaction would have added ambiguity to the coordination number determination. A more troublesome competing reaction can arise when the proton affinity of a site in a metal complex is very similar to the proton affinity of the reagent ligand. In such a case, the reaction might result in stabilization of a proton-bound complex. Collisional stabilization of such proton-bound species can be facilitated by the relatively high pressure of He that is present in the QITMS during the experiment. Distinguishing between proton-mediated addition and metal-mediated addition is difficult, so without insight into the chemical nature of the metal-bound ligand, an incorrect coordination number could be assigned. In our experience, choosing a good titrating ligand with a low gas-phase basicity, such as acetonitrile, allows the proton-bound products and proton transfer reactions to be avoided.

3.1.2. Ligand-donor groups

Another reaction that can be competitive with ligand addition is ligand-group displacement, and this reaction can be difficult to avoid. Ligand-group displacement can occur when a functional group in a ligand is bound to the metal relatively weakly. An example of such a reaction is illustrated by the data in Fig. 4. When Co(II) complexes of the two ligands shown in Fig. 5 are reacted with acetonitrile for 100 ms, the reactions proceed to noticeably different extents despite each ligand having five donor groups. The Co(II) complex of DIEN-$(THF)_2$ reacts as expected for a 5-coordinate complex to add just a single acetonitrile, whereas the DIEN-$(fur)_2$ complex adds two acetonitriles. In the latter case, acetonitrile probably displaces one of the furan groups that are weakly bound to Co(II). Furan binds to Co(II) mainly via weak π interactions [54,55], whereas the tetrahydrofuran group of DIEN-$(THF)_2$ binds to Co(II) via a stronger σ interaction. This σ interaction makes ligand displacement much less favorable. In general, we have found that the titration experiments are effective for determining the coordination number of complexes when the ligand-donor groups are good σ donors, regardless of the donating heteroatom. For example, the coordination numbers of complexes with thioether and/or ether functionality can be successfully determined as long as there is strong σ character to their bonding as opposed to π character [14,28]. Of course, the σ-bonding capacity of a functional group can vary significantly, and so in some cases, ligand-group displacement can still occur to a small extent if the reaction is allowed to proceed long enough. Fig. 6 shows an example of this with a kinetic plot of the reaction of acetonitrile with $Co(DIEN\text{-}(THF)_2)^{2+}$. If this reaction is

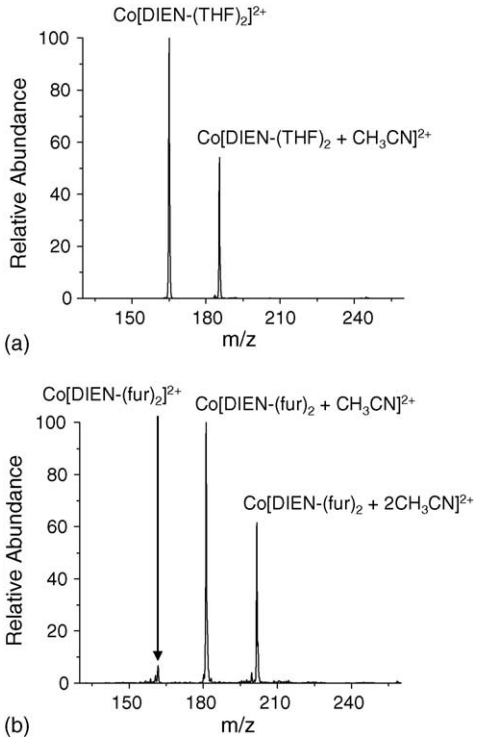

Fig. 4. Mass spectra obtained after reacting: (a) $Co[DIEN\text{-}(THF)_2]^{2+}$ and (b) $Co[DIEN\text{-}(fur)_2]^{2+}$ with acetonitrile (pressure = $4.2 \pm 0.4 \times 10^{-10}$ atm) for 100 ms.

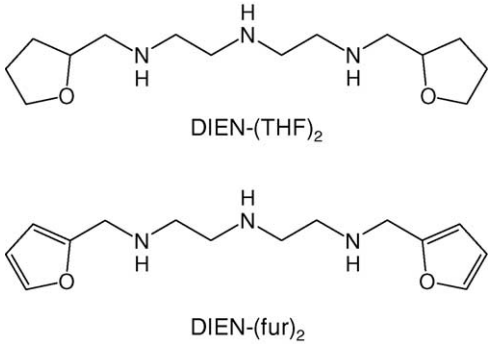

Fig. 5. Ligand structures for complexes whose reaction data are shown in Fig. 4.

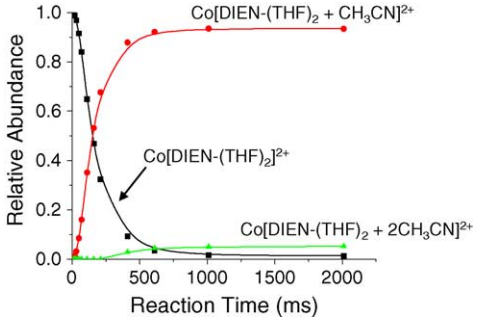

Fig. 6. Kinetic plot for the association reaction of $Co[DIEN\text{-}(THF)_2]^{2+}$ with acetonitrile (pressure = $4.2 \pm 0.4 \times 10^{-10}$ atm).

allowed to reach equilibrium, a second acetonitrile will add to the complex, but its relative abundance is below 5%. As far as coordination number determinations are concerned, we typically choose an arbitrary threshold of 20% relative abundance for determining whether a ligand addition reaction is indicative of coordinative unsaturation. This arbitrary level is based upon our experience with >100 complexes of known coordination numbers. So, while this level is a useful operational threshold for our experiments, it is not clearly rooted in any properties of divalent metal–ligand complexes or reagent ligands, nor is it tied to any obvious instrumental parameter.

3.1.3. Metal center

As mentioned earlier, using a titration reaction to determine coordination number relies on solution- and solid-phase observations that indicate the tendency of divalent metal complexes to form 6-coordinate complexes; however, this tendency is not equal for all metal ions. Table 2 shows the equilibrium constants for the reactions of acetonitrile ($4.2 \pm 0.4 \times 10^{-10}$ atm) with the Mn(II), Fe(II), Co(II), Ni(II), Cu(II) and Zn(II) complexes of DIEN-$(pyr)_2$. The general trend in equilibrium constants is Ni(II) > Mn(II) > Fe(II) > Co(II) > Cu(II), Zn(II). What explains these differences in reactivity? One possible explanation might be found in the 18-electron rule, which states that stable metal complexes will be those that attain a total of 18 electrons in their valence shell upon acquiring electrons from ligand-donor groups. This would seem to explain the low reactivity of the Cu(II) and Zn(II) complexes, which have 9 and 10 d-electrons, respectively, and so are not expected to readily form 6-coordinate complexes upon reaction with acetonitrile. Assuming that the five nitrogen donors of DIEN-$(pyr)_2$ are each 2-electron donors and acetonitrile is a 2-electron donor, then the 6-coordinate complexes of Cu(II) and Zn(II) would have 21 and 22 electrons, respectively. One might then conclude that any reactions observed with the Cu(II) and Zn(II) complexes are due to ligand displacement reactions or are due to an interaction between acetonitrile and the metal-bound ligand, both of which are not very favorable.

A difficulty with invoking the 18-electron rule comes when trying to explain the results with Ni[DIEN-$(pyr)_2$]$^{2+}$, which reacts more extensively than all other complexes shown in Table 2. According to the 18-electron rule, Ni[DIEN-$(pyr)_2$]$^{2+}$ should be fairly unreactive as the addition of acetonitrile results in a total of 20 valence electrons (8 from Ni(II), 10 from DIEN-$(pyr)_2$, 2 from acetonitrile). In the case of the Ni(II) complexes, ligand-donor group displacement or an acetonitrile–ligand interaction are not attractive explanations because the reaction with acetonitrile happens so readily. The ligand-donor groups in DIEN-$(pyr)_2$ are expected to interact strongly with the metal, thus lowering the tendency for ligand-group displacement. Also, an interaction between acetonitrile and DIEN-$(pyr)_2$ is expected to be very weak and metal independent. The 18-electron formalism then is probably not the best way to explain the trends observed in Table 2, and furthermore, we feel its general utility for complexes between first-row metals and ligands with good σ donors is very minimal, although its applicability for ligands that are π acceptors is more definite. Indeed, the 18-electron rule is known to fail altogether when first-row metals are complexed to bipyridine ligands [56], which are very good σ donors. Also, a search of the Cambridge Structural Database shows that about 50% of Ni(II) complexes, 30% of Cu(II) complexes and 20% of Zn(II) complexes are 6-coordinate [57], which further suggests the low applicability of the 18-electron rule for such complexes.

So, what explains the trend in reactivity observed in Table 2? In recent work [58], we showed that the trend can be explained by calculating molecular orbital stabilization energies (MOSE) using the angular overlap model (AOM). The AOM can be used to obtain the energy separation of the metal d-orbitals for any symmetrical complex structure while taking into account σ and π interactions, metal spin-state and metal complex geometry [59–61]. MOSE values in terms of σ- (e_σ) and/or π-orbital overlap integrals (e_π) can be determined using molecular orbital energy level diagrams like those shown in Fig. 7. MOSE values can be separately obtained for 5- and 6-coordinate

Table 2
Equilibrium constants determined experimentally and molecular orbital stabilization energies (MOSE) calculated from the angular overlap model for M[DIEN-$(pyr)_2$]$^{2+}$ complexes reacting with acetonitrile (pressure of $4.2 \pm 0.4 \times 10^{-10}$ atm)

Metal (M)	Equilibrium constant[a] ($\times 10^{10}$ atm^{-1})	ΔMOSE (σ)[b] (e_σ)	ΔMOSE (σ + π)[c] (e_σ)
Mn	19 ± 7	−1	−2
Fe	5 ± 2	−1	−1.67
Co	0.7 ± 0.3	−1	−1.33
Ni	33 ± 15	−2.125	−2.125
Cu	0.21 ± 0.05	−0.25	−0.25
Zn	0.14 ± 0.07	0	0

[a] Equilibrium constants for the addition of a single acetonitrile.

[b] These MOSE values are calculated by only considering the σ interactions between the metal and the ligand and are calculated by considering a high-spin trigonal bipyramidal complex reacting to form a high-spin octahedral complex. The values are listed in terms of the σ-overlap integrals (e_σ), which are assumed to be the same for each metal in each coordination environment.

[c] These MOSE values are calculated by considering the σ interactions between the metal and the ligand and the π interactions between the metal and acetonitrile. These values are calculated by considering a high-spin trigonal bipyramidal complex reacting to form a high-spin octahedral complex. The values are given in terms of σ-overlap integrals (e_σ) for simplicity. The magnitude of the π-overlap integral (e_π) is assumed to be 1/12 of the magnitude of the sigma overlap integral (i.e. $e_\pi/e_\sigma = 0.083$).

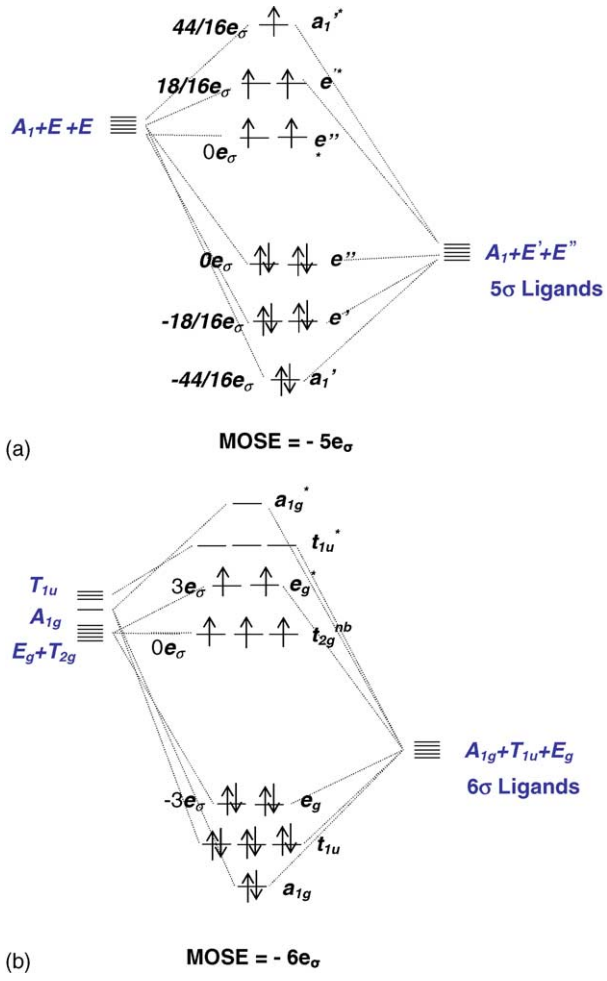

Fig. 7. Molecular orbital energy level diagrams for: (a) a high-spin trigonal bipyramidal complex of Mn(II) and (b) a high-spin octahedral complex of Mn(II), considering in both cases only the σ contributions from the ligand. The molecular orbital stabilization energy (MOSE) is determined by summing the appropriate σ-orbital overlap integrals for each filled or partially filled orbital.

complexes of each metal after considering all possible spin states, geometries and combinations of σ and π interactions. Changes in MOSE (ΔMOSE) can then be calculated and compared to the experimentally determined ΔG values, which are estimated from the equilibrium constants shown in Table 2. Just as a more negative ΔG value corresponds to a more favorable reaction, a more negative ΔMOSE value also corresponds to a more favorable reaction. In determining the MOSE values, the overlap integrals were assumed to be the same for each metal, which should be a fairly valid assumption given the identical ligand in each complex.

Upon considering all the numerous possible geometries, spin states and donor interactions, the qualitative trend in Table 2 can be explained by considering that each metal complex reacts from a high-spin trigonal bipyramidal state to form a high-spin octahedral complex [58]. The Cu(II) and Zn(II) complexes gain essentially no stabilization upon adding acetonitrile, whereas the Ni(II) complex and to lesser extents the Mn(II), Fe(II) and Co(II) complexes are stabilized by the addition of acetonitrile (Table 2). The significant stabilization observed in the Ni(II) complex arises from the unfavorable electron configuration associated with a high-spin trigonal bipyramidal structure relative to a high-spin octahedral structure. Interestingly, the relative reactivity of the Mn(II), Fe(II) and Co(II) complexes can be explained by recognizing that the interaction of acetonitrile with these complexes has a subtle, yet important, π character (see Table 2). The d_{xy}, d_{yz} and d_{xz} orbitals of these metals have favorable symmetry (t_{2g}) to overlap with the p orbitals of acetonitrile, and so the partially filled character of these orbitals for Mn(II) (t_{2g}^3), Fe(II) (t_{2g}^4) and Co(II) (t_{2g}^5) in an octahedral environment results in additional stabilization that is not seen in the Ni(II), Cu(II) or Zn(II) complexes. This additional stabilization follows the trend Mn(II) > Fe(II) > Co(II), and as such the Mn(II) complex reacts more extensively than the Fe(II) and Co(II) complexes.

3.1.4. Coordination number determination—summary

In summary, I–M reactions of divalent metal complexes have the potential to provide coordination number by using a reagent gas to titrate open coordination sites on a metal, but several factors affect reactivity such that one must be careful when interpreting the results. The coordination number determination is based upon a binary result—reaction or no reaction. This result is convenient analytically, but the identity of the reagent gas used, the nature of the bonding between the metal and ligand-donor atoms and the electronic structure of the metal center can all affect the outcome of the reaction.

3.2. Types of coordinating functional groups

A simple increase in *m*/*z* ratio after reaction of a divalent metal complex ion with a reagent ligand provides a mass spectrometric response that provides insight into a complex's coordination number, but kinetic and thermodynamic data can provide additional information. The chemical nature of the ligand-groups bound to a metal ion exerts an important influence on the reactivity of that metal by tuning its electronic structure. Indeed, the coordination structure around a metal ion is of interest because of this tuning. The kinetics and thermodynamics of a metal complex reaction should reflect the chemical nature of the functional groups bound to the metal ion. This idea was demonstrated recently for a series of 5-coordinate complexes of Co(II) and Ni(II) with the ligands shown in Fig. 8 [14]. If these complexes are reacted with acetonitrile for varying time periods, then data like that shown in Fig. 9 is generated. From this data, both equilibrium and rate constants can be extracted (Table 3). Fig. 9 and Table 3 clearly show that changes to the ligand functional groups bound to a given metal lead to significant changes in reactivity.

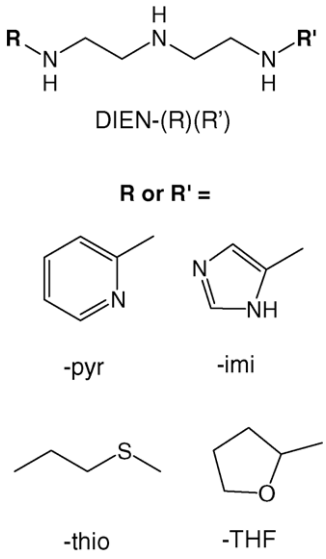

Fig. 8. Ligands used to generate the data that are shown in Table 3.

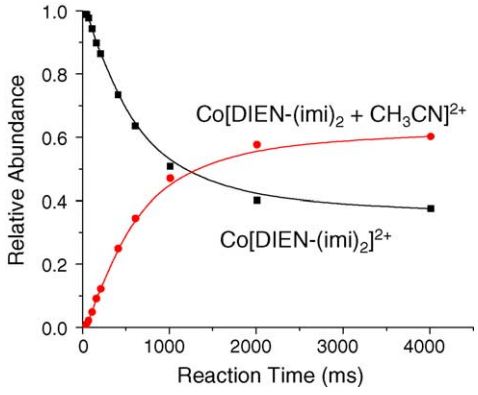

Fig. 9. Kinetic plot for the association reaction of $Co[DIEN\text{-}(imi)_2]^{2+}$ with acetonitrile (pressure = $4.2 \pm 0.4 \times 10^{-10}$ atm).

Because acetonitrile adduct formation occurs via an association reaction, both the equilibrium and rate constants in Table 3 reflect the binding strength of acetonitrile to a given complex. The overall observed reaction is shown in Eq. (1).

The equilibrium constant is

$$M[DIEN-(R)(R')]^{2+} + CH_3CN \underset{k_r}{\overset{k_f}{\rightleftarrows}} M[DIEN-(R)(R')+CH_3CN]^{2+} \quad (1)$$

related to ΔG of the reaction, and because ΔS is similar in every case, the equilibrium constant predominantly reflects the product–reactant enthalpy difference, to which the main contribution is acetonitrile binding. Our contention that the reaction rate reflects acetonitrile binding strength can be understood by considering the dynamics of association reactions. Because association reactions are generally considered to occur via a two-step process (Eqs. (2) and (3)), the forward reaction rate constant (k_f) reflects several reaction characteristics. An important

$$M[DIEN-(R)(R')]^{2+} + CH_3CN \underset{k_b}{\overset{k_a}{\rightleftarrows}} (M[DIEN-(R)(R')]+CH_3CN)^{*2+} \quad (2)$$

$$(M[DIEN-(R)(R')]+CH_3CN)^{*2+} \underset{k_{ac}[He]}{\overset{k_s[He]}{\rightleftarrows}} M[DIEN-(R)(R')+CH_3CN]^{2+} \quad (3)$$

characteristic that affects k_f is the lifetime of the excited intermediate, which is controlled by the relative rates of dissociation (k_b) and stabilization. Stabilization of the intermediate can occur via collisions with He and/or radiative emission. The relatively high pressure of He ($\sim 1 \times 10^{-4}$ Torr) in the QITMS suggests that collisional stabilization plays a more important role than radiative stabilization. Indeed, from recent experiments in which the He pressure was varied, we have estimated that the contribution from radiative stabilization of the intermediate is only about 1% under our reaction conditions [Leeson, Vachet, unpublished]. Considering only collisional stabilization and invoking the steady-state approximation, we can determine k_f

$$k_f = \frac{k_a k_s[He]}{k_b + k_s[He]} \quad (4)$$

Table 3
Association rate and equilibrium constants for the addition of one acetonitrile to various Co(II) and Ni(II) complexes (pressure of acetonitrile = $4.3 \pm 0.4 \times 10^{-10}$ atm)

Ligand	Rate constants ($\times 10^{-10}$ cm^3 molecule^{-1} s^{-1})		Equilibrium constants ($\times 10^{10}$ atm^{-1})	
	Co(II)	Ni(II)	Co(II)	Ni(II)
$DIEN\text{-}(THF)_2$	6 ± 1	10 ± 1	50 ± 15	>60[a]
DIEN-(THF)(thio)	4.1 ± 0.6	8.1 ± 0.1	31 ± 6	>60[a]
$DIEN\text{-}(thio)_2$	3.5 ± 0.4	5.9 ± 0.9	2.3 ± 0.5	>60[a]
DIEN-(THF)(pyr)	3 ± 1	–	18 ± 7	–
DIEN-(THF)(imi)	2.8 ± 0.1	5.8 ± 0.1	15 ± 5	>60[a]
$DIEN\text{-}(pyr)_2$	2.3 ± 0.4	4.5 ± 1.0	0.7 ± 0.3	33 ± 15
DIEN-(thio)(pyr)	1.7 ± 0.2	–	1.12 ± 0.07	–
$DIEN\text{-}(imi)_2$	1.0 ± 0.3	2.5 ± 0.9	0.33 ± 0.05	1.0 ± 0.4
DIEN-(thio)(imi)	0.8 ± 0.2	2.3 ± 0.2	0.29 ± 0.02	2.1 ± 0.9

[a] Equilibrium constants above 6.0×10^{11} atm^{-1} are difficult to confidently determine with our mass spectrometer.

(Eq. (4)) as a function of the rate constants shown in Eqs. (2) and (3). Because the complexes in Table 3 are all similar in size and the initial encounters between the divalent metal complex ion and acetonitrile are controlled by ion–dipole interactions, k_a is expected to be similar for all complexes. This assumes that every acetonitrile–metal complex encounter leads to the excited intermediate. Also, the collisional stabilization term, k_s[He], is expected to be similar for each complex as it is controlled by ion-induced dipole interactions. Thus, differences in the magnitude of k_b directly control the experimentally measured differences in k_f (rate constants in Table 3). The magnitude of k_b is described by RRKM theory, and its magnitude is inversely proportional to the acetonitrile binding strength.

The data shown in Table 3 generally indicate that metal complexes with more nitrogen donor groups bind acetonitrile more weakly than complexes with sulfur or oxygen donor groups. For example, the Co(II) complex of DIEN-(imi)$_2$ with its low equilibrium and rate constants binds acetonitrile more weakly than the Co(II) complexes of DIEN-(thio)$_2$ or DIEN-(THF)$_2$. An explanation for this observation can be found by considering the Hard and Soft Acid and Base (HSAB) principle [62]. The HSAB principle states that hard acids (i.e. metal ions) more favorably interact with hard bases (i.e. ligand-donor groups), and soft acids more favorably interact with soft bases. According to the HSAB principle Co(II) and Ni(II) are borderline acids and thus interact more favorably with borderline bases such as pyridine and imidazole groups. Oxygen-containing groups are classified as hard bases, and sulfur-containing groups are typically classified as soft bases. Thus, the interactions between Co(II) or Ni(II) and the nitrogen-containing bases (e.g. pyridine and imidazole) are more favorable than the interactions with either the hard (e.g. THF) or soft (e.g. thioether) bases. The more favorable interactions result in more electron density on the metal and thus weaker acetonitrile binding.

Interestingly, the acetonitrile binding strengths for complexes having a mix of nitrogen-, oxygen- and/or sulfur-containing groups indicate that the effects of different groups are additive somewhat. For example, the equilibrium constants for Co[DIEN-(THF)$_2$]$^{2+}$ and Co[DIEN-(thio)$_2$]$^{2+}$ are $50 \pm 15 \times 10^{10}$ and $2.3 \pm 0.5 \times 10^{10}$ atm^{-1}, respectively, while at $31 \pm 6 \times 10^{10}$ atm^{-1} the equilibrium constant for Co[DIEN-(THF)(thio)]$^{2+}$ is almost the average of the two. Analytically speaking, this additive effect is encouraging because it would suggest that one might be able determine the number and type of each functional group in a complex by reacting it with acetonitrile (or other suitable reagent) and measuring the reaction rate or equilibrium constant. One might envision a collection of complexes that act as a calibration set. By comparing the reactivity of an unknown complex to this calibration set, the identity and number of different functional groups bound to the metal could be determined.

While our results are generally consistent with the HSAB principle and the effect of different donor groups on acetonitrile binding strength is somewhat additive, some exceptions are observed. The exceptions, though, provide some interesting insight into the intrinsic chemistry of the complexes that react anomalously. From the data in Table 3, the reactivity of the complexes of DIEN-(imi)(thio) are most clearly inconsistent. The equilibrium constant for Co[DIEN-(imi)(thio)]$^{2+}$, for example, would be expected to fall between the equilibrium constants of Co[DIEN-(imi)$_2$]$^{2+}$ and Co[DIEN-(thio)$_2$]$^{2+}$, but in fact the value for this complex is the lowest of all the Co(II) complexes. In previous work [14], we argued that this was do to the "softening" of the metal center by the presence of a strongly interacting imidazole group, which makes the interaction with the soft base thioether more favorable. Because the hard and soft descriptors are related to the polarizability of a metal or donor group, extensive electron donation by imidazole to Co(II) makes the metal more polarizable (i.e. "softer"). While this exception weakens the analytically utility of I–M reactions, it does provide an example of some new insight into coordination chemistry that is available from such gas-phase reactions.

3.3. Reagent gas considerations

Information about the coordinating functional groups that is available from the I–M reactions depends on the nature of the reagent gas and the experimental He pressure. The differences in reactivity shown in Table 3 basically arise from the different magnitudes of k_b in Eq. (2). If k_b is very small relative to k_s[He], then the observed formation constant, k_f, will approach the value of k_a (see Eq. (4)). The magnitude of k_a is essentially the collision rate constant between the complex ion and reagent gas, which is mostly dependent upon ion–dipole interactions between the ion and the neutral reagent. In other words, k_a contains essentially no information about the coordination structure of the metal complex. So, if the He pressure is too high or the reagent gas forms a very strong adduct with the metal complex such that k_b is small, then the results of the I–M reactions will not reflect the functional groups bound to the metal.

An example of improper reagent gas usage is a set of experiments in which acetonitrile is reacted with a series of 4-coordinate Zn complexes (Table 4 and Fig. 10). Acetonitrile forms such a strong adduct with these 4-coordinate

Table 4
Association rate and equilibrium constants for the addition of one acetonitrile to several Zn(II) complexes (pressure of acetonitrile = $4.3 \pm 0.4 \times 10^{-10}$ atm)

Ligand	Rate constants ($\times 10^{10}$ cm^3 molecule^{-1} s^{-1})	Equilibrium constants ($\times 10^{10}$ atm^{-1})
EN-(THF)(imi)	23 ± 3	>60[a]
EN-(pyr)(NH$_2$)	22 ± 2	>60[a]
EN-(imi)(NH$_2$)	19 ± 2	>60[a]
EN-(pyr)(imi)	19 ± 1	>60[a]
EN-(pyr)$_2$	15 ± 3	>60[a]

[a] Equilibrium constants above 6.0×10^{11} atm^{-1} are difficult to confidently determine with our mass spectrometer.

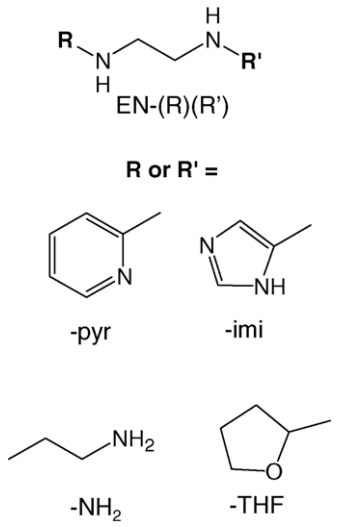

Fig. 10. Ligands used to generate the data that are shown in Table 4.

complexes that all the equilibrium constants for the addition of a single acetonitrile exceed values that can be confidently measured with our experimental setup. In addition, the rate constants approach the collision rate for each of the complexes, and so the measured rate constants are very similar despite significant differences in the coordinating functional groups. The solution to this problem is to use a reagent gas, such as ammonia, that binds the Zn complexes less avidly.

3.3.1. Coordinating functional group determination—summary

In summary, the kinetics and thermodynamics of adduct formation reactions in the gas-phase are influenced by the functional groups bound to a given divalent metal ion. Not surprisingly, the reaction extent is related to how effectively a given functional group can donate electron density to the metal center. For divalent first-row metals, nitrogen-containing groups are more effective than sulfur- or oxygen-containing functional groups at donating electron density, and so divalent metal complexes with nitrogen donors are the least reactive with reagent ligands. This observation is consistent with the HSAB principle. The significant differences in reactivity that are observed for the divalent metal complexes as a function of the ligand-donor groups suggest that I–M reactions in a mass spectrometer could be used analytically to provide some insight into the groups bound to a metal ion. Such an approach, however, would likely require development of a sufficient reaction database of known complexes for comparison with unknown complexes.

3.4. Coordination geometry

The spatial arrangement of ligand-donor groups around a transition metal can have a significant effect on the chemistry of a given metal center, and so this information is useful when characterizing a metal complex. This influence on

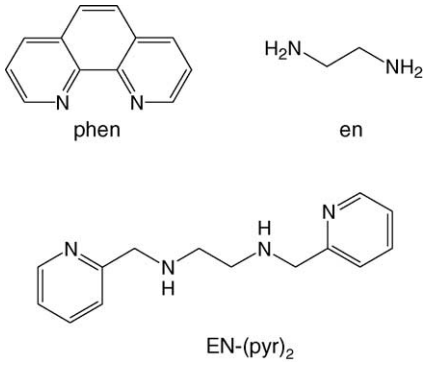

Fig. 11. Ligands used to generate the data that are shown in Tables 5 and 6.

metal chemistry arises because different ligand arrangements produce different energy splitting patterns for the normally degenerate five d-orbitals. The relationship between the d-orbital splitting patterns and orbital occupancy can lead to interesting chemical reactivity, magnetic properties and/or redox properties. Thus, just as changes to ligand functional groups exert an influence on gas-phase reactivity, so might changes to coordination geometry exert an influence on gas-phase reactivity.

As an illustration of how coordination geometry can influence gas-phase reactivity, we recently reported the significant changes in reactivity undergone by 4-coordinate Ni(II) complexes as the ligand set is changed [63]. Consider the Mn(II), Co(II) and Ni(II) complexes of the three ligands shown in Fig. 11. The donor-groups in these ligands are not substantially different, so they are not expected to lead to significant changes in complex reactivity, and in fact the equilibrium constants for the reactions of the Mn(II) and Co(II) complexes with NH_3 are fairly similar (Table 5). For Ni(II), however, the equilibrium constant for $Ni(phen)_2^{2+}$ is three to four orders of magnitude higher than the equilibrium constants of the other two Ni(II) complexes.

The reason for the significant change in the equilibrium constant becomes evident upon considering the coordination geometry of each of the Mn(II), Co(II) and Ni(II) complexes. Density functional theory (DFT) calculations using the B3LYP method with the LANL2DZ basis set, which contains effective core potentials, was used to generate geometry optimized structures for each of the complexes represented in Table 5. Fig. 12 shows the geometry optimized structures of $Ni[EN\text{-}(pyr)_2]^{2+}$ and $Ni(phen)_2^{2+}$ to illustrate some struc-

Table 5
Equilibrium constants for the reactions of $M(EN\text{-}(pyr)_2)^{2+}$, $M(en)(phen)^{2+}$ and $M(phen)_2^{2+}$ complexes with NH_3 (pressure of $NH_3 = 2.6 \pm 0.1 \times 10^{-9}$ atm)

Metal (M)	Equilibrium constants[a] ($\times 10^{10}$ atm^{-1})		
	EN-$(pyr)_2$	(en)(phen)	$(phen)_2$
Mn	1.4 ± 0.7	3 ± 2	5 ± 3
Co	1.1 ± 0.4	1.9 ± 0.6	0.3 ± 0.1
Ni	0.002 ± 0.001	0.03 ± 0.01	12 ± 4

[a] Equilibrium constants for the addition of a single NH_3.

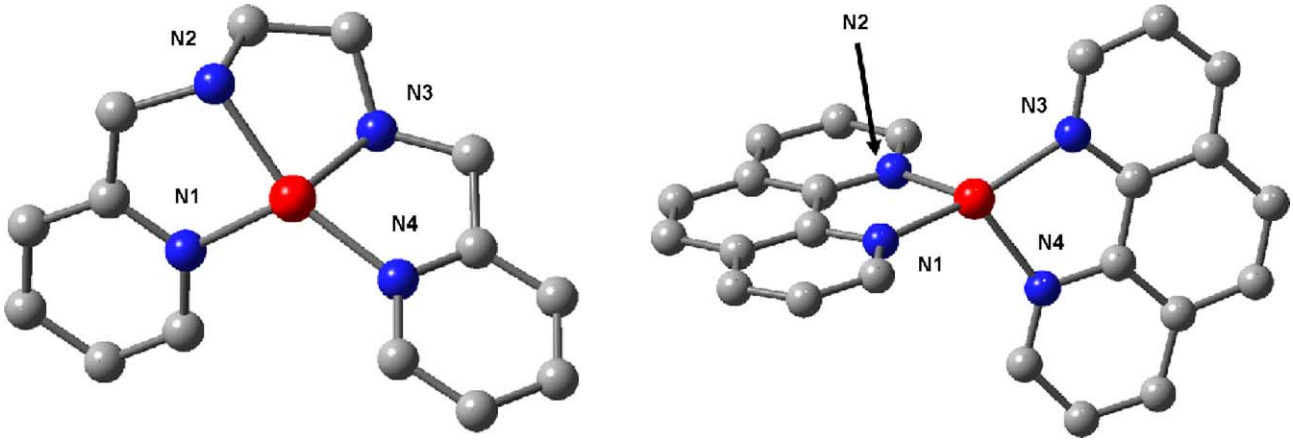

Fig. 12. DFT geometry optimized structures of Ni[EN-$(pyr)_2$]$^{2+}$ (left) and Ni$(phen)_2^{2+}$ (right).

tural features of the complexes. Four-coordinate complexes have two idealized geometries—square planar and tetrahedral. A convenient means of characterizing the degree to which a given 4-coordinate complex represents one of these geometries is to consider the dihedral angle between the two planes containing the metal and two of the cis donor atoms. In Fig. 12, one plane consists of the metal and nitrogens N1 and N2, and the other plane consists of the metal and nitrogens N3 and N4. For perfectly tetrahedral complexes the dihedral angle is 90°, and for perfectly square planar complexes the dihedral angle is 0°. The dihedral angles for each of the complexes in Table 5 are listed in Table 6. Clearly, each of the Mn(II) and Co(II) complexes are predominantly tetrahedral, but the coordination geometry of the Ni(II) complexes depends on the ligands around the metal. The Ni(II) complexes of EN-$(pyr)_2$ and (en)(phen) are square planar, and the more highly reactive Ni$(phen)_2^{2+}$ is tetrahedral. The tetrahedral geometry of the Ni$(phen)_2^{2+}$ complex is likely enforced by steric interactions between hydrogens on the C2 and C9 positions of the phen groups. These steric interactions prevent d^8 Ni(II) from adopting its preferred square planar coordination geometry.

Table 6
Dihedral angles for M(EN-$(pyr)_2)^{2+}$, M(en)$(phen)^{2+}$ and M$(phen)_2^{2+}$ complexes, which were obtained from the DFT optimized structures

Metal (M)	Dihedral angles[a] (°)		
	EN-$(pyr)_2$	(en)(phen)	$(phen)_2$
Mn	76.3	73.7	72.0
Co	73.1	75.6	74.5
Ni	29.1[b]	4.1[b]	68.0

[a] The dihedral angles are for the two planes containing the metal and two of the cis donor atoms. One plane consists of the metal and nitrogens N1 and N2 (from Fig. 12), and the other plane consists of the metal and nitrogens N3 and N4 (Fig. 12). For perfectly tetrahedral complexes the dihedral angle is 90°, and for perfectly square planar complexes the dihedral angle is 0°.

[b] The lowest energy structures for these complexes are low-spin. The lowest energy structures for all other complexes are high-spin.

The DFT calculations clearly indicate differences in coordination geometries for the three Ni(II) complexes, but why is the tetrahedral complex of Ni(II) so much more reactive than the square planar complexes of this metal? To answer this question, we again calculated MOSE using the same procedure described earlier. Table 7 shows the ΔMOSE values obtained for various coordination geometries and spin states for Mn(II), Co(II) and Ni(II). Three conclusions can be drawn from the MOSE calculations. First, low-spin square planar complexes of Ni(II) are not expected to react extensively to form high-spin 5-coordinate complexes of either geometry (i.e. D_{3h} or C_{4v}) as indicated by ΔMOSE values of $1e_\sigma$ and

Table 7
The change in the molecular orbital stabilization energies (ΔMOSE) calculated from the angular overlap model for the conversion of a 4-coordinate complex to a 5-coordinate complex considering all possible geometries and spin states but only σ contributions from the ligands and NH_3

	ΔMOSE (e_σ)[a]			
	$D_{4h} \rightarrow C_{4v}$[b]	$D_{4h} \rightarrow D_{3h}$[b]	$T_d \rightarrow C_{4v}$[b]	$T_d \rightarrow D_{3h}$[b]
High-spin ML_4 to high-spin ML_5				
Mn	−1	−1	−1	−1
Co	−1	−1	−1	−1
Ni	−1	0.125	−2.33	−1.21
Low-spin ML_4 to low-spin ML_5				
Mn	−2	−0.88	−3.33	−2.21
Co	−1	0.37	−4	−2.63
Ni	0	0.5	−3.33	−2.83
Low-spin ML_4 to high-spin ML_5				
Mn	3	3	1.67	1.67
Co	2	2	−1	−1
Ni	1	2.12	−2.33	−1.21
High-spin ML_4 to low-spin ML_5				
Mn	−6	−4.88	−6	−4.88
Co	−4	−2.63	−4	−2.63
Ni	−2	−1.5	−3.33	−2.83

[a] The ΔMOSE values are given in terms of σ-overlap integrals (e_σ).

[b] D_{4h}, square planar; C_{4v}, square pyramidal; T_d, tetrahedral; D_{3h}, trigonal bipyramidal.

$2.12e_\sigma$. This explains the low reactivity of the Ni(II) complexes of EN-$(pyr)_2$ and (en)(phen) (see Table 5). The lowest energy structures for these complexes are low-spin square planar according to the DFT calculations (Table 6). Furthermore, most 5-coordinate complexes of first-row transition metals having ligands with good σ donors are high-spin [64], so the product ion is likely a high-spin complex.

A second conclusion from the data in Table 7 is that high-spin tetrahedral complexes of Ni(II) are expected to react extensively to form high-spin 5-coordinate complexes of either geometry (i.e. D_{3h} or C_{4v}) as indicated by ΔMOSE values of $-2.33e_\sigma$ and $-1.21e_\sigma$. This prediction is in accord with the experimental and calculated data for $Ni(phen)_2^{2+}$. The experimentally measured equilibrium constant for this complex is the highest of those shown in Table 5, and the DFT calculations indicate that the lowest energy conformer of this species is a high-spin tetrahedral complex.

A third conclusion from the data in Table 7 is that high-spin tetrahedral complexes of Mn(II) and Co(II) are expected to react favorably to form high-spin 5-coordinate complexes of either geometry (i.e. D_{3h} or C_{4v}). ΔMOSE values of $-1e_\sigma$ for both Mn(II) and Co(II) indicate this expectation. Interestingly, tetrahedral complexes of Mn(II) and Co(II) are expected to react less extensively than tetrahedral Ni(II) complexes, and in fact this is observed experimentally.

The ΔMOSE values in Table 7 also allow other predictions to be made about the gas-phase reactivity of divalent metal complexes. For example, square planar complexes of Co(II) are expected to be fairly unreactive. Square planar complexes of Co(II) are invariably low-spin because of the relatively high energy of the d_{x2-y2} and d_{xy} orbitals, and a ΔMOSE value of $2e_\sigma$ is calculated for the conversion of a low-spin square planar complex to a high-spin 5-coordinate complex. To see if this prediction holds, a Co(II) complex of cyclam (Fig. 13) and a Co(II) complex with two ethylenediamine (en) ligands were reacted with ammonia. The measured equilibrium constants were 0.009×10^{10} and 0.9×10^{10} atm^{-1} for $Co(cyclam)^{2+}$ and $Co(en)_2^{2+}$, respectively. The equilibrium constant for $Co(cyclam)^{2+}$, which is a square planar complex, is two orders of magnitude lower than the equilibrium constant of the $Co(en)_2^{2+}$ complex, which has essentially the same ligand-donor groups but a different coordination geometry.

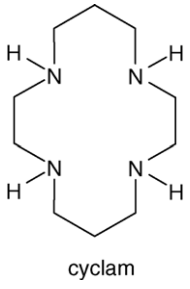

Fig. 13. Structure of cyclam (1,4,8,11-tetraazacyclotetradecane).

In summary, the coordination geometry around a given metal ion influences the d-orbital splitting patterns for that metal, which in turn influences its chemistry. Gas-phase reactions are sensitive to these changes in d-orbital energy levels such that square planar and tetrahedral complexes of metals such as Ni(II) and Co(II) react to noticeably different extents. MOSE calculations provide a convenient means of explaining this reactivity and predicting how coordination geometry in general will affect metal complex reactivity.

3.5. The effect of steric interactions

In the previous sections of this review, we have demonstrated that divalent metal complex ions react in ways that reflect their coordination number, coordinating functional groups and coordination geometry. While this is true in many cases, steric effects can conceal the correlations between reactivity and coordination structure in other cases. Because the information content available from I–M reactions comes from reagent gas binding to the metal, steric effects that impact either the approach or the effective binding of the reagent to the metal center will minimize the information that is available.

The following two examples illustrate the impact that sterics can have on the gas-phase reactivity of metal complexes. First, Fig. 14 shows plots of the reactions of acetonitrile with $Ni[DIEN\text{-}(pyr)_2]^{2+}$ and $Ni[DIEN\text{-}(2\text{-}Me\text{-}pyr)_2]^{2+}$. These two complexes differ only by the presence of methyl groups

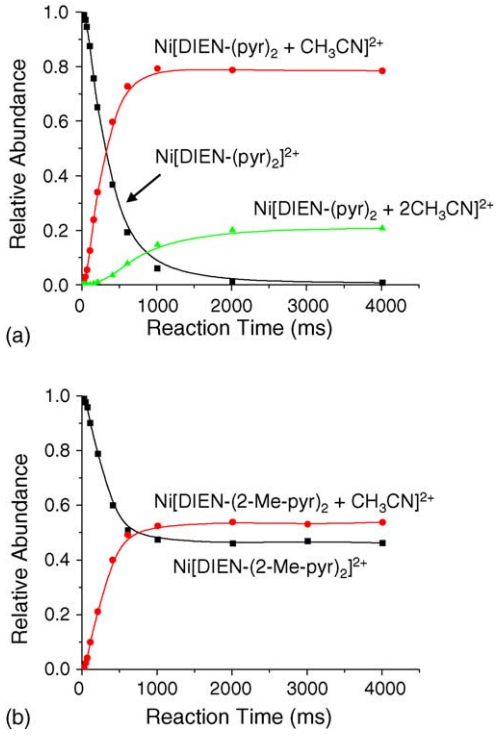

Fig. 14. Kinetic plots for the association reactions of (a) $Ni[DIEN\text{-}(pyr)_2]^{2+}$ and (b) $Ni[DIEN\text{-}(2\text{-}Me\text{-}pyr)_2]^{2+}$ with acetonitrile (pressure = $4.2 \pm 0.4 \times 10^{-10}$ atm).

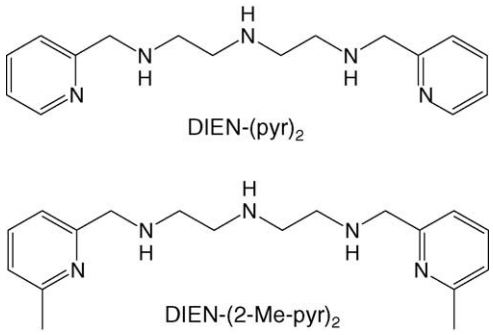

Fig. 15. Ligands used to generate the data that are shown in Fig. 14.

on the two position of each pyridine ring (Fig. 15), but the extent of reaction is noticeably different in each case [65]. Steric hindrance by the methyl group circled in Fig. 16 causes acetonitrile to bind less favorably to Ni[DIEN-(2-Me-pyr)$_2$]$^{2+}$. In the geometry optimized structure of the acetonitrile adduct, Ni[DIEN-(2-Me-pyr)$_2$+CH_3CN]$^{2+}$ (structure not shown), acetonitrile binds trans to N2, which is clearly hindered by the presence of the methyl group indicated in Fig. 16. Another possible explanation for the less favorable reaction of Ni[DIEN-(2-Me-pyr)$_2$]$^{2+}$ is electron donation by the methyl groups on the pyridine rings, which would cause the pyridine nitrogens to donate electron density more effectively to the metal. This effect is expected to be small, however, given that methyl groups are weak electron donors. We find it unlikely that such a weak inductive effect would decrease the measured equilibrium constant by a factor of ~150 (from 33×10^{10} to 0.23×10^{10} atm^{-1}).

An even more obvious example of steric effects can be seen in a comparison of the reactions of acetonitrile with Ni(4,7-dmphen)$_2^{2+}$ and Ni(2,9-dmphen)$_2^{2+}$, where 4,7-dmphen is 4,7-dimethylphenanthroline and 2,9-dmphen is 2,9-dimethylphenanthroline (Fig. 17). Both of these complexes are high-spin tetrahedral species, and based upon MOSE calculations shown earlier (Table 7), these complexes should be very reactive. Indeed, Ni(4,7-dmphen)$_2^{2+}$ is very reactive with an equilibrium constant for the addition of one acetonitrile that is too high to confidently determine with our instrument setup. Furthermore, a second acetonitrile readily adds to this species as expected for a four-coordinate complex. In contrast, however, Ni(2,9-dmphen)$_2^{2+}$ is essentially unreactive with acetonitrile. After 4000 ms, no ion corresponding to the acetonitrile adduct of Ni(2,9-dmphen)$_2^{2+}$ is observed. The very low reactivity of this complex is most easily explained by considering the methyl groups in the C2 and C9 positions of the phenanthroline rings. These methyl groups prevent the approach of acetonitrile to the metal center and may also make it difficult for the complex to reorganize to accommodate the acetonitrile ligand.

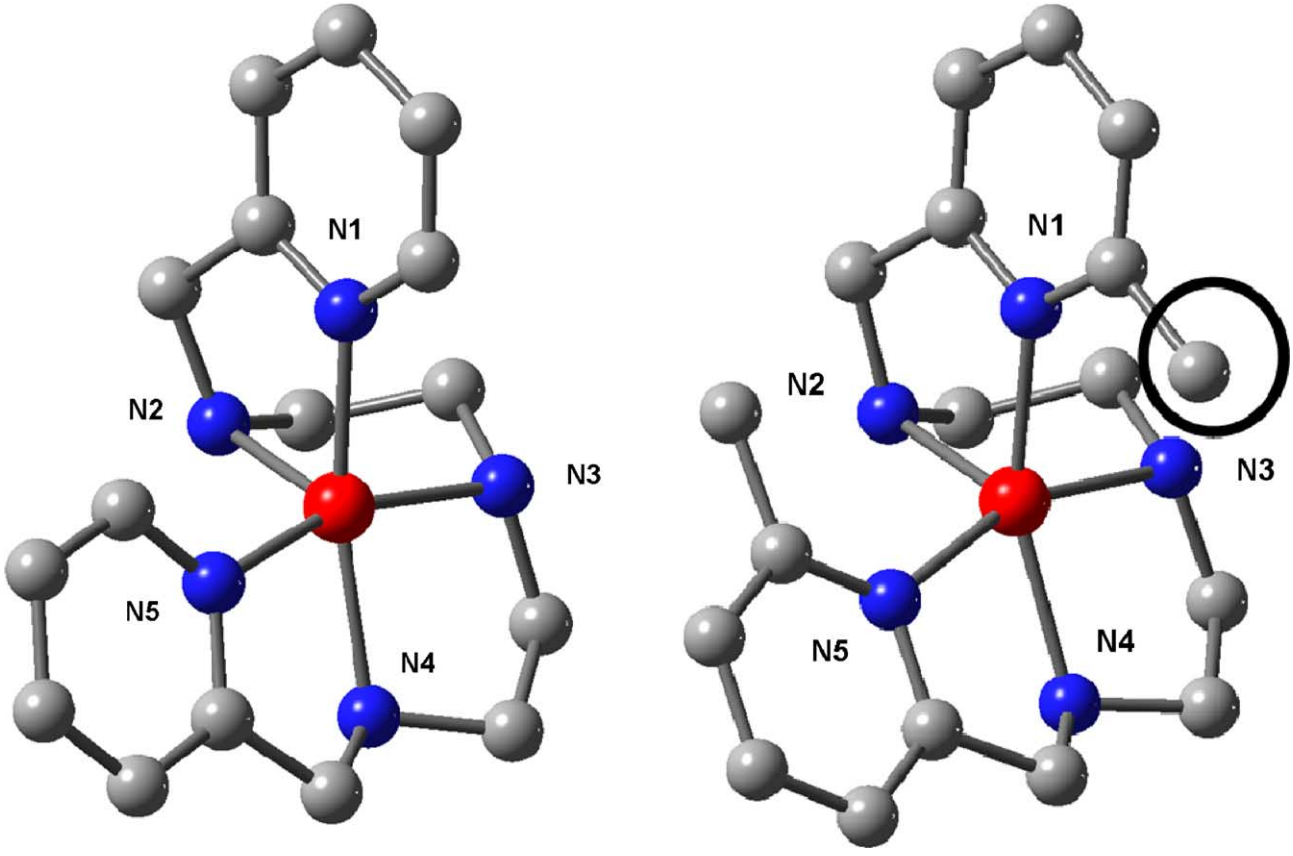

Fig. 16. DFT geometry optimized structures for the Ni complexes of the DIEN-(pyr)$_2$ (left) and DIEN-(2-Me-pyr)$_2$ (right). In the acetonitrile adducts of these complexes, acetonitrile binds to the metal trans to N2. In the structure on the right the circled methyl group sterically interferes with the addition of acetonitrile.

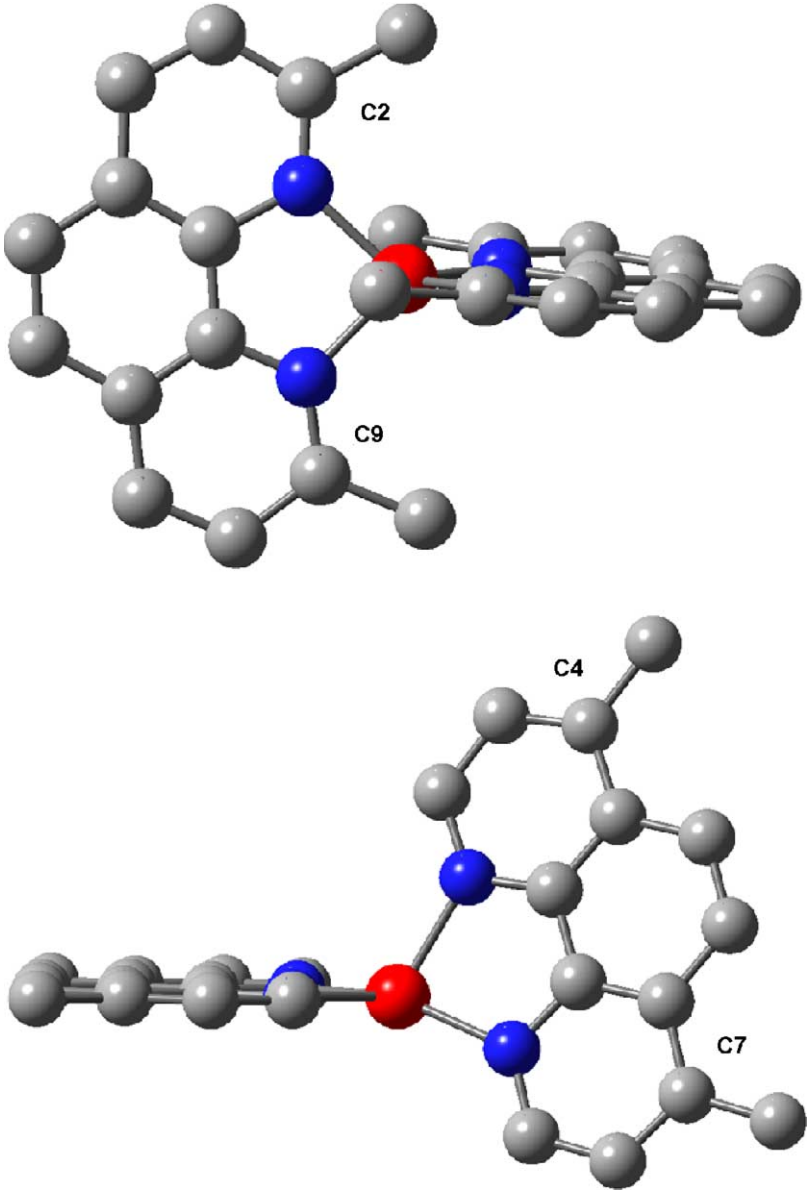

Fig. 17. DFT geometry optimized structures of Ni(2,9-dmphen)$_2^{2+}$ (top) and Ni(4,7-dmphen)$_2^{2+}$ (bottom).

4. Concluding remarks

Gas-phase I–M reactions of divalent metal complex ions are noticeably affected by the coordination structure around the metal ion. Thus, from an analytical perspective, I–M reactions may have the potential to provide coordination structure information for such complexes. I–M reactions seem to give information than is not accessible from typical analytical CID experiments that are performed on commonly used mass spectrometers. The extent of a complex's reactivity with a neutral reagent molecule is dependent on the coordination number of the complex, the type of functional groups bound to the metal and the geometry of the ligands around the metal ion. Gas-phase dissociation experiments of divalent metal complexes have yet to show a clear connection to such properties. The general analytical utility of these I–M reactions still remains to be seen, but such an approach appears to be useful for relatively small divalent metal–ligand complexes like the ones illustrated in this report. Investigations into the reactivity of a wider variety of metal–ligand complexes are necessary to more fully establish the value of this approach. In the very least, I–M reactions of divalent metal complex ions will provide structural information that is complementary to analytical CID experiments. In comparison to threshold CID measurements, which are currently limited to monovalent metal complex ions, I–M reactions in a QITMS may not provide as detailed and precise thermodynamic information, but they do provide access to coordination structure information

and some thermodynamic information using less-specialized equipment. In addition, because analytical CID experiments are readily performed in a QITMS along with I–M reactions, the complementary information provided by these two methods may offer access to more diverse information than is possible with threshold CID measurements.

Even if such I–M reactions are only analytically useful under special circumstances, gas-phase reactions of coordinatively unsaturated metal complex ions have the potential to provide some fundamentally interesting information. Many catalytic intermediates contain coordinatively unsaturated metal ions, and the ability to study such short-lived species in the controlled environment of a mass spectrometer could lead to greater insight into a catalyst's chemistry. Obtaining information about the coordination structure of such intermediates might give important insight into how coordination structure controls the chemical transformations that these species undergo.

Acknowledgement

This work was sponsored by the Office of Naval Research under Award No. N000140010796.

References

[1] P. Hu, M.L. Gross, J. Am. Chem. Soc. 115 (1993) 8821.
[2] A. Reiter, J. Adams, H. Zhao, J. Am. Chem. Soc. 116 (1994) 7827.
[3] G. Hopfgartner, C. Piguet, J.D. Henion, J. Am. Soc. Mass Spectrom. 5 (1994) 748.
[4] P. Hu, J.A. Loo, J. Am. Chem. Soc. 117 (1995) 11314.
[5] C.L. Gatlin, F. Turecek, T. Vaisar, J. Am. Chem. Soc. 117 (1995) 3637.
[6] E.J. Alvarez, H-F. Wu, C.C. Liou, J. Brodbelt, J. Am. Chem. Soc. 118 (1996) 9131.
[7] C.L. Gatlin, F. Tureček, in: R.B. Cole (Ed.), Electrospray Ionization Mass Spectrometry, JohnWiley & Sons, New York, 1997, p. 527.
[8] E.J. Alvarez, V.H. Vartanian, J.S. Brodbelt, Anal. Chem. 69 (1997) 1147.
[9] M.T. Rodgers, P.B. Armentrout, Mass Spectrom. Rev. 19 (2000) 215.
[10] P.B. Armentrout, J. Mass Spectrom. 200 (2000) 219.
[11] M.T. Rodgers, J. Phys. Chem. A 105 (2001) 2374.
[12] P.B. Armentrout, J. Am. Soc. Mass Spectrom. 13 (2002) 419.
[13] M.T. Rodgers, P.B. Armentrout, Acc. Chem. Res. 37 (2004) 989.
[14] M.Y. Combariza, R.W. Vachet, J. Am. Soc. Mass Spectrom. 13 (2002) 813.
[15] H-F. Wu, J.S. Brodbelt, Inorg. Chem. 34 (1995) 615.
[16] R.W. Vachet, J.R. Hartman, J.H. Callahan, J. Mass Spectrom. 33 (1998) 1209.
[17] G.E. Reid, R.A.J. O'Hair, M.L. Styles, W.D. McFadyen, R.J. Simpson, Rapid Commun. Mass Spectrom. 12 (1998) 1701.
[18] R.K. Milburn, V. Baranov, A.C. Hopkinson, D.K. Bohme, J. Phys. Chem. A 102 (1998) 9803.
[19] R.K. Milburn, V. Baranov, A.C. Hopkinson, D.K. Bohme, J. Phys. Chem. A 103 (1999) 6373.
[20] R.K. Milburn, M.V. Frash, A.C. Hopkinson, D.K. Bohme, J. Phys. Chem. A 104 (2000) 3926.
[21] J.R. Hartman, R.W. Vachet, J.H. Callahan, Inorg. Chim. Acta 297 (2000) 79.
[22] R.W. Vachet, J.H. Callahan, J. Mass Spectrom. 35 (2000) 311.
[23] R.W. Vachet, J.R. Hartman, J.W. Gertner, J.H. Callahan, Int. J. Mass Spectrom. 204 (2001) 101.
[24] V. Baranov, D.K. Bohme, Int. J. Mass Spectrom. 210/211 (2001) 303.
[25] B.A. Perera, M.P. Ince, E.R. Talaty, M.J. Van Stipdonk, Rapid Commun. Mass Spectrom. 15 (2001) 615.
[26] B.A. Perera, A.L. Gallardo, J.M. Barr, S.M. Tekarli, V. Anbalagan, E.R. Talaty, M.J. Van Stipdonk, J. Mass Spectrom. 37 (2002) 401.
[27] J.R. Hartman, R.W. Vachet, W. Pearson, R.J. Wheat, J.H. Callahan, Inorg. Chim. Acta 343 (2003) 119.
[28] M.Y. Combariza, R.W. Vachet, Anal. Chim. Acta 496 (2003) 233.
[29] D. Hanna, M. Silva, J. Morrison, S. Tekarli, V. Anbalagan, M. Van Stipdonk, J. Phys. Chem. A 107 (2003) 5528.
[30] A.K. Gianotto, B.D.M. Hodges, M.T. Benson, P.D. Harrington, A.D. Appelhans, J.E. Olson, G.S. Groenewold, J. Phys. Chem. A 107 (2003) 5948.
[31] G.L. Gresham, A.K. Gianotto, P.D. Harrington, L.B. Cao, J.R. Scott, J.E. Olson, A.D. Appelhans, M.J. Van Stipdonk, G.S. Groenewold, J. Phys. Chem. A 107 (2003) 8530.
[32] W. Chien, V. Anbalagan, M. Zandler, M. Van Stipdonk, D. Hanna, G. Gresham, G. Groenewold, J. Am. Soc. Mass Spectrom. 15 (2004) 777.
[33] A.K. Vrkic, T. Taverner, P.F. James, R.A.J. O'Hair, Dalton Trans. (2004) 197.
[34] J.R. Hartman, M.Y. Combariza, R.W. Vachet, Inorg. Chim. Acta 357 (2004) 51.
[35] J.R. Hartman, A.L. Kammier, R.J. Spracklin, W.H. Pearson, M.Y. Combariza, R.W. Vachet, Inorg. Chim. Acta 357 (2004) 1141.
[36] D.E. Goeringer, K.G. Asano, S.A. McLuckey, Int. J. Mass Spectrom. 182/183 (1999) 275.
[37] K.G. Asano, D.E. Goeringer, S.A. McLuckey, Int. J. Mass Spectrom. 185/186/187 (1999) 207.
[38] K.G. Asano, D.E. Goeringer, D.J. Butcher, S.A. McLuckey, Int. J. Mass Spectrom. 190/191 (1999) 281.
[39] A.T. Blades, P. Jayaweera, M.G. Ikonomou, P. Kebarle, J. Chem. Phys. 92 (1990) 5900.
[40] A.T. Blades, P. Jayaweera, M.G. Ikonomou, P. Kebarle, Int. J. Mass Spectrom. Ion Proc. 102 (1990) 251.
[41] C.A. Woodward, M.P. Dobson, A.J. Stace, J. Phys. Chem. A 101 (1997) 2279.
[42] A.J. Stace, N.R. Walker, S. Firth, J. Am. Chem. Soc. 119 (1997) 10239.
[43] N.R. Walker, R.R. Wright, P.E. Barran, H. Cox, A.J. Stace, J. Chem. Phys. 114 (2001) 5562.
[44] R.R. Wright, N.R. Walker, S. Firth, A.J. Stace, J. Phys. Chem. A 105 (2001) 54.
[45] C.J. Thompson, J. Husband, F. Aguirre, R.B. Metz, J. Phys. Chem. A 104 (2000) 8155.
[46] K.P. Faherty, C.J. Thompson, F. Aguirre, J. Michne, R.B. Metz, J. Phys. Chem. A 105 (2001) 10054.
[47] A.A. Shvartsburg, J. Am. Chem. Soc. 124 (2002) 12343.
[48] A.A. Shvartsburg, Chem. Phys. Lett. 360 (2002) 479.
[49] T.D. Burns, T.G. Spence, M.A. Mooney, L.A. Posey, Chem. Phys. Lett. 258 (1996) 669.
[50] T.G. Spence, T.D. Burns, L.A. Posey, J. Phys. Chem. A 101 (1997) 139.
[51] T.G. Spence, T.D. Burns, G.B. Guckenberger, L.A. Posey, J. Phys. Chem. A 101 (1997) 1081.
[52] K.J. Miller, J.A. Savchik, J. Am. Chem. Soc. 101 (1979) 7206.
[53] G. Innorta, L. Pontoni, S. Torroni, J. Am. Soc. Mass Spectrom. 9 (1998) 314.
[54] D.L. Kershner, F. Basolo, Coord. Chem. Rev. 70 (1987) 279.
[55] B. Chaudret, F.A. Jalon, J. Chem. Soc., Chem. Commun. (1988) 711.
[56] F.A. Cotton, G. Wilkinson, C.A. Murillo, M. Bochmann, Advanced Inorganic Chemistry, sixth ed, John Wiley & Sons, New York, 1999.

[57] D. Venkataraman, Y. Du, S.R. Wilson, P. Zhang, K. Hirsch, J.S. Moore, J. Chem. Ed. 74 (1997) 915.
[58] M.Y. Combariza, J.T. Fermann, R.W. Vachet, Inorg. Chem. 43 (2004) 2745.
[59] C.K. Jorgensen, R. Pappalardo, H.H. Schmidtke, J. Chem. Phys. 39 (1963) 1422.
[60] C.E. Schaffer, C.K. Jorgensen, Mol. Phys. 9 (1965) 401.
[61] C.E. Schaffer, Pure Appl. Chem. 24 (1970) 361.
[62] R.G. Pearson, J. Am. Chem. Soc. 85 (1963) 3533.
[63] M.Y. Combariza, R.W. Vachet, J. Phys. Chem. A 108 (2004) 1757.
[64] R. Morassi, I. Bertini, L. Sacconi, Coord. Chem. Rev. 8 (1972) 351.
[65] M.Y. Combariza, R.W. Vachet, J. Am. Soc. Mass Spectrom. 15 (2004) 1128.